1. Andrii Bereziuk[1], 2. Oleksiy Karlov [2], 3. Roman Kryshchuk[2], 4. Ihor Garasymchuk[3], 5. Pavlo Potapskyi[3],6. Mykola Vusatyi [3]

The National University of Life and Environmental Sciences of Ukraine (1), Podilsky State Agrarian and Technical University (3)
The Institute of Electrodynamics of the National Academy of Sciences of Ukraine (2),
ORCID: 1. 0000-0003-0305-5894, 2. 0000-0002-1350-1870; 3. 0000-0002-1933-0144; 4. 0000-0002-4304-4447;5. 0000-0003-4792-8992; 6. 0000-0003-3070-9283

doi:10.15199/48.2021.07.09

Energy parameters of induction heat generator with branched heat exchanger for production of environmentally friendly coolant

***Abstract**. A comparative analysis of the results of numerical modelling of electro physical processes occurring in the middle of a cylindrical inductor, using different configurations of the heat exchanger has been proved. According to the results of computer simulation, a comparison of power, resistance, inductance and current at given values of the electromotive force at the terminals of the inductor winding was done.*

***Streszczenie.** Przeprowadzono analizę porównawczą wyników modelowania numerycznego procesów elektrofizycznych zachodzących w środku wzbudnika cylindrycznego przy zastosowaniu różnych konfiguracji wymiennika ciepła. Zgodnie z wynikami symulacji komputerowej dokonano porównania mocy, rezystancji, indukcyjności i prądu przy zadanych wartościach siły elektromotorycznej na zaciskach uzwojenia cewki indukcyjnej. (**Parametry energetyczne indukcyjnego generatora ciepła z rozgałęzionym wymiennikiem ciepła do wytwarzania ekologicznie czystego nośnika ciepła**).*

Keywords: induction heating, cylindrical inductor, energy parameters, drying of raw materials.
Słowa kluczowe: nagrzewanie indukcyjne, wzbudnik cylindryczny, parametry energetyczne, suszenie surowców.

Introduction

In the technological processes of processing biomass of plant origin, there is often a need to heat it [1], for example, in the manufacture of granular or briquette biofuels. Heat treatment can also be used in the preparation of seed, preparation of various feeds, drying of agricultural products, fluids etc. [2,3].

For traditional methods of heat treatment of materials of plant origin are mainly used devices in which heat generation is carried out by burning various types of mineral or organic fuels, accompanied by harmful emissions into the environment and air pollution. Also widespread are installations in which the coolant is obtained by converting electrical energy - resistive heating. This method of transferring heat energy to the heat exchanger is not safe and reliable enough.

One of the promising and safe ways to heat a heat exchange device is an induction method of energy transfer [4], in which heating is carried out by inducing eddy currents. The metal parts of the heat exchanger structure (heating elements) are heated according to Joule's law, followed by heat transfer (convection and radiation) to the heat carrier (for example air).

Induction heating has a number of advantages: high flux density of electromagnetic energy; the ability to achieve the required temperatures in the coolant (in a fairly wide range); the heating process is environmentally friendly; the ability to control the temperature distribution through design solutions, changes in the modes of operation of induction equipment (frequency, supply voltage); high efficiency. Disadvantages include reactive power compensation.

To analyze the energy performance of induction heaters for various purposes, it is necessary to perform mathematical modeling of electromagnetic fields [5-6]. In the analysis of the electromagnetic field in a ferromagnetic medium with nonlinear magnetic permeability, the numerical finite element method has become the most widespread today, on the basis of which there are many computer programs for modeling the electromagnetic field and other physical processes [7,8].

In the design of an inductor with a cylindrical winding and internal loading of term heat sources, the electromagnetic flow passes inside the winding cylinder through the heating elements and is closed from the outside of the inductor through the air space (Fig. 1,a). Since the heating elements are made of steel, they also act as a magnetic circuit. In order to improve the energy performance of the inductor, it is proposed to use heating ferromagnetic elements outside the inductor (Fig. 1,b-e). Therefore, it is proposed to place the heating elements in the middle of the cylindrical winding and outside, which may affect the improvement of energy performance.

The aim of article is to establishing the influence on the energy parameters of the induction heat generator of different designs of the branched heat exchanger.

To calculate the electromagnetic field, the finite element method and the three-dimensional formulation of the problem are used.

Electromagnetic field equation for quasi-stationary mode:

$$div\mathbf{B} = 0\,,\ rot\mathbf{H} = \mathbf{j}\,,\ rot\mathbf{A} = \mathbf{B}\,,$$

(1) $$\mathbf{E} = -\frac{\partial \mathbf{A}}{\partial t} - grad\varphi\,,\ \mathbf{B} = \mu\mathbf{H}\,,\ \mathbf{j} = \sigma\mathbf{E}$$

where $\mathbf{A}$, $\mathbf{B}$, $\mathbf{H}$, $\mathbf{j}$ – vectors of magnetic vector potential, magnetic induction, magnetic field strength, current density accordingly; σ – electrical conductivity; t – time, φ – electric scalar potential, μ – magnetic permeability. For harmonic currents, equations (1) change as follows:

$$div\hat{\mathbf{B}} = 0\,,\ rot\hat{\mathbf{H}} = \hat{\mathbf{j}}\,,\ rot\hat{\mathbf{A}} = \hat{\mathbf{B}}\,,$$

(2) $$\hat{\mathbf{E}} = -i\omega\hat{\mathbf{A}} - grad\varphi\,,\ \hat{\mathbf{B}} = \mu\hat{\mathbf{H}}\,,\ \hat{\mathbf{j}} = \sigma\hat{\mathbf{E}}$$

where $\hat{\mathbf{A}}$, $\hat{\mathbf{B}}$, $\hat{\mathbf{H}}$, $\hat{\mathbf{j}}$ – complex amplitudes of magnetic vector potential, magnetic induction, magnetic field strength, current density accordingly, ω - angular frequency, i – imaginary unit.

Electromagnetic field equations for a three-dimensional model from a system of equations (2):

(3) $$rot\left(\frac{rot\hat{\mathbf{H}}}{\sigma}\right) = -i\omega\hat{\mathbf{B}} + rot\left(\frac{\hat{\mathbf{j}}_S}{\sigma}\right)$$

Herein $\hat{\mathbf{j}}_S$ – the complex amplitude of the current density of the power supply, which is present in the cross section of the winding. The value $\hat{\mathbf{j}}_S$ is calculated on the findings given voltage winding and complex resistance induction system.

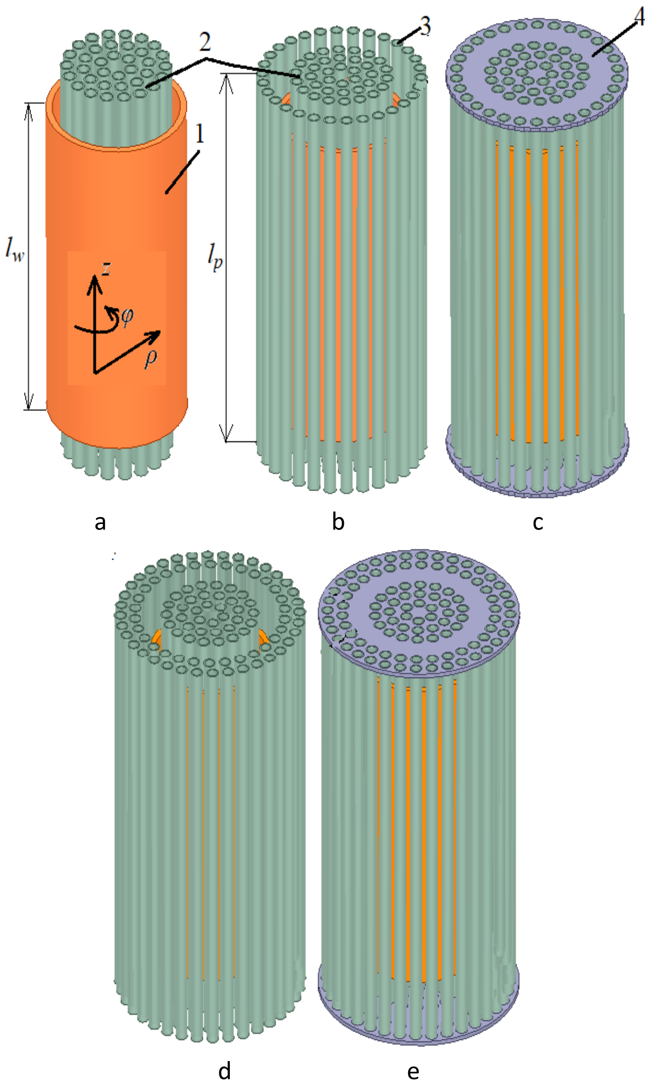

Fig. 1. Different models of the induction system

Model for research

Fig. 1 presents drawings of three-dimensional models of the induction system for modeling parameters and energy performance by the finite element method. Fig. 1 presents the following models: induction system with the placement of ferromagnetic tubes inside the cylindrical coil (Fig. 1,a); with the placement of ferromagnetic tubes both inside and outside the cylindrical coil (Fig. 1,b-e); with the presence of ferromagnetic boards at the ends of the induction system (Fig. 1,c,e). Thus, the parameters and energy parameters of five structures of the induction system (Fig. 1), as well as the sixth structure (Fig. 1,c*) with charged ferromagnetic boards are studied.

Fig. 1 has the following designations: 1 - inductor winding; 2 - bundles of ferromagnetic tubes (term heat sources) located inside the winding; 3 - bundles of ferromagnetic tubes outside the winding; 4 - ferromagnetic boards with holes for pipes.

In order to reduce the size of the calculations, the calculation of the symmetrical 1/12 part of the induction system is performed, as shown in Fig. 2 (Fig. 1,a), and then after calculating the electromagnetic field, the parameters (power, resistance and inductance) are multiplied by 12. The electromotive force at the terminals of the winding is 12 times smaller. At the boundaries of symmetry with the normal coordinate φ of the cylindrical coordinate system (ρ, φ, z - Fig. 1) the boundary condition of symmetry with tangential magnetic flux is given, and at the boundary of symmetry with the normal coordinate z - with normal magnetic flux.

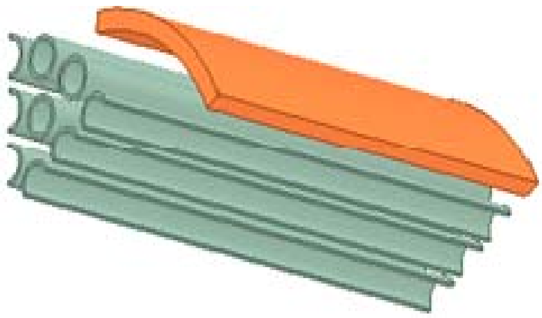

Fig. 2. Symmetrical 1/12 part of the induction system

The dimensions of the induction system are set for the study: the length of the cylindrical winding l_w – 780 mm; length of ferromagnetic tubes l_p – 995 mm (Fig. 1); inner and outer diameters of the winding - 320 mm and 352 mm; inner and outer diameters of ferromagnetic tubes - 27.1 mm and 33.5 mm; diameters of ferromagnetic boards - 480 mm (with one layer of external pipes, Fig. 1,b-c) and 560 mm (with two layers of external pipes, Fig. 1,d-e); thickness of ferromagnetic boards l_{pp} – 10 mm.

The winding conductors are made of a rectangular copper tube 14x16 mm with a wall thickness of 2 mm, cross section 104 mm^2. Given 48 turns, the resistance of the DC winding at a given conductivity of 58 MSm/m is R_w = 8,4 mOhm. AC resistance coefficient of the winding with conductors-tubes and a current frequency of 50 Hz will not have a significant impact on the result of the study and therefore it is not taken into account to simplify the electromagnetic problem. Ferromagnetic tubes are made of steel with an electrical conductivity of 2,1 MSm/m, taking into account the magnetization curve. The magnetization curve for the calculation is chosen as in JFE Steel 35JNE250. Ferromagnetic boards have such parameters as ferromagnetic tubes.

In modeling, eddy currents are induced in ferromagnetic tubes and boards. Only a given current density is present in the winding, and therefore equation (3) has the form:

(4) $$rot\left(\frac{rot\hat{\mathbf{H}}}{\sigma}\right)=rot\left(\frac{\hat{\mathbf{j}}_S}{\sigma}\right).$$

In the ferromagnetic parts of the induction system, equation (3) has the following form:

(5) $$rot\left(\frac{rot\hat{\mathbf{H}}}{\sigma}\right)=-i\omega\hat{\mathbf{B}}.$$

In the air:

(6) $$rot\left(\frac{rot\hat{\mathbf{H}}}{\sigma}\right)=0.$$

At the internal boundaries of the media, the boundary condition of equality of the normal components of induction and the tangential components of the magnetic field strength is adopted. At the outer boundary is the boundary condition of zero of the normal component of the magnetic field strength.

The calculation of the electromagnetic field begins with the model presented in Fig. 1,a. Here the amplitude value of voltage U_m=311 V (effective value 220 V, 50 Hz) is set. When modeling 1/12 of the induction system, the voltage and resistance of the winding are set as 1/12: U_m/12=25,92 V, R_w/12=0,7 mOhm. The results of the calculation are listed in table 1 with the designation of the column «Fig. 1,a».

The table shows the following parameters of the induction system: Um – the amplitude value of the voltage on the induction system; $\mathcal{E}_m$ – the electromotive force on the winding terminals; I_m – the amplitude value of the current in the winding; P_2 – the power in the pipes; P_p – the power in the boards; P_w – the power in the winding; P – total power; S – total full power; cos(φ) – the power factor; R – the active resistance of the induction system; L – the inductance of the induction system; Ψ – flux coupling; B_{mn} – the average amplitude value of magnetic field induction in internal heat term elements; B_{mn2} – the average amplitude value of magnetic field induction in external heating elements; Bmn3 – the average amplitude value of magnetic field induction in boards.

The calculations results and their analysis

The name of the column «Fig. 1,c*» means the presence of charged ferromagnetic boards.

Table 1 Parameters of the induction system

Param.	Fig. 1,a	Fig. 1,b	Fig. 1,c	Fig. 1,c*	Fig. 1,d	Fig. 1,e
$\lvert U_m \rvert$, V	311,00	311,27	311,68	311,33	311,15	311,55
$\lvert \mathcal{E}_m \rvert$, V	310,52					
$\lvert I_m \rvert$, A	548,25	377,67	326,10	269,58	342,51	282,64
P_2, W	8213,5	13543,2	15569,8	14679,6	11245,2	12946,8
P_p, W	–	–	5580,24	–	–	5954,4
P_w, W	1262,4	599,1	446,63	305,24	492,73	335,52
P, W	9575,9	14142,3	21596,6	14984,8	11737,9	19236,7
$\lvert S \rvert$, VA	85254,2	58779,1	50819,0	41964,1	53285,8	44029,1
cos(φ)	0,112	0,241	0,425	0,357	0,220	0,437
R, mOhm	63,71	198,29	406,20	412,38	200,09	481,61
L, mH	1,79	2,55	2,75	3,43	2,82	3,16
$\lvert \Psi \rvert$, Vb	0,984	0,962	0,898	0,926	0,966	0,892
B_{mn}, T	1,81	1,78	1,87	1,90	1,78	1,87
B_{mn2}, T	–	1,61	1,79	1,77	1,23	1,42
B_{mn3}, T	–	–	1,57	1,31	–	1,40

When performing the calculation in all cases, the same value of the electromotive force $\mathcal{E}_m$ was set in order to obtain the maximum equal value of the magnetic field in the induction system. Since the electrical losses in the winding are much smaller than in the heating elements, so in all cases, the supply voltage U_m varies within 1 V (Table 1). The values of flux coupling *Ψ* and magnetic field induction in internal heat term elements differ by no more than 10%.

There are 36 ferromagnetic tubes inside the winding (Fig. 1,a). Outside the winding, there are two options - 30 pipes (Fig. 1,b,c) and 66 pipes (Fig. 1,d,e). As shown in Table 1, the presence of heat term elements around the winding can significantly reduce the current in the winding: when using one row of pipes outside the winding (Fig. 1,b), the current decreased by 31%, and in the presence of two rows of pipes (Fig. 1,d) - by 38%. In the presence of massive ferromagnetic boards (Fig. 1,c,e), the current decreased by 40% and 48%, accordingly, compared with Fig. 1,a. When comparing the inductor with massive ferromagnetic boards (Fig. 1,c) and with charge (Fig. 1,c*), the current with charge boards is lower by 17%. The inductor with the charged boards (Fig. 1,c*) in comparison with a variant without external pipes (Fig. 1,a) has on 50% less current.

Comparing the losses in the winding (table 1), the use of additional external heat term elements led to a reduction of losses by 52… 75% (Fig. 1,b-e).

When using external heating elements with one row of pipes (Fig. 1,b), the power increased by 65%, and with two rows of pipes (Fig. 1,d) - by 37% (Tab. 1). When using ferromagnetic solid boards - 89% and 57%, accordingly. In addition, ferromagnetic solid boards also emit significant power, which is 64% (Fig. 1,c) and 54% (Fig. 1,e) less, respectively, compared with the power in the heating elements (Tab. 1). This shows that there is an optimal number of pipes that can be installed outside the winding to maximize the power of the induction system. In this case, a larger total power in the heat term elements is obtained with one row of external ferromagnetic tubes (Fig. 1,c and c*).

When we use stacked ferromagnetic boards (Fig. 1,c*), the power in the heat term elements became 5.7% less (Fig. 1,c and c*), but the current decreased by 17.3%. At the same time boards do not heat up and carry out a role of a magnetic circuit (Fig. 1, c*). In order for air to pass not only in the ferromagnetic tubes, but also in the air gaps between the tubes, you can make holes in the ferromagnetic boards. This design of ferromagnetic boards in the form of a «snowflake» was studied in [9]. The study of the influence of pipe boards in the article [9] showed that the design of pipe boards in the form of a «snowflake» of solid unstitched material can reduce losses in them by more than 10 times.

Visually, the ratio of the values of active and total power released in different types of models of induction systems can be seen in the diagram (Fig. 3).

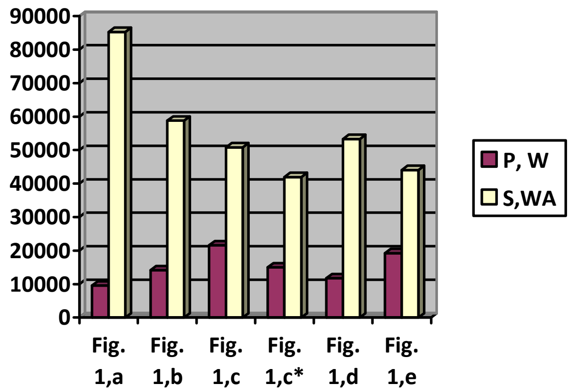

Fig. 3. Diagram of different types of models of induction systems

Conclusion

When using additional external heat term elements in the design of the induction system with a cylindrical winding for biomass drying, it is possible to increase the useful power by 65… 89%, reduce the current in the winding by 31… 50%.

The use of additional ferromagnetic solid tubular boards with holes for heating elements allows to increase the useful power by an additional 15%, but the boards have significant losses (36-46% of the losses in the heat term elements).

The use of stacked ferromagnetic solid boards allows to increase the useful power by 8% (compared to without boards) and in stacked boards the losses will be low.

***Authors**: Andrii Bereziuk, candidate of technical sciences, docent of Department of Electrical Engineering, Electromechanics and Electrotechnology, National University of Life and Environmental Sciences of Ukraine, Geroev Oboroni str., 15, Kyiv, 03041, Ukraine, E-mail: marshall241987@gmail.com; Oleksiy Karlov, candidate of technical sciences, senior researcher of the Department of Electromagnetic Systems of the Institute of Electrodynamics of the NAS of Ukraine, prospekt Peremogy, 56, Kiev, 03680, Ukraine, E-mail: lexa.k.ua@gmail.com; Roman Kryshchuk, candidate of technical sciences, researcher of the Department of Electromagnetic Systems of the Institute of Electrodynamics of the NAS of Ukraine, prospekt Peremogy, 56, Kiev, 03680, Ukraine, E-mail: kr@nas.gov.ua; Ihor Garasymchuk, candidate of technical sciences, Head of Department of Electrical Engineering, Electromechanics and Electrotechnologies, Educational and Scientific Institute of Energy, Podilsky State Agrarian and Technical University, Shevchenko Str, 13, Kamianets-Podilskyi, 32316, Ukraine, E-mail: igorgarasymchuk@gmail.com; Pavlo Potapskyi, candidate of technical sciences, docent of Department of Electrical Engineering, Electromechanics and Electrotechnologies, Educational and Scientific Institute of Energy, Podilsky State Agrarian and Technical University, Shevchenko Str, 13, Kamianets-Podilskyi, 32316, Ukraine, E-mail: p.v.potap@meta.ua; Mykola Vusatyi, assistant of Department of Electrical Engineering, Electromechanics and Electrotechnologies, Educational and Scientific Institute of Energy, Podilsky State Agrarian and Technical University, Shevchenko Str, 13, Kamianets-Podilskyi, 32316, Ukraine, E-mail: 0611142015vys@gmail.com.*

REFERENCES

[1] Zablodskiy M, Zhiltsov A, Kondratenko I, Gritsyuk V, Conception of efficiency of heat electromechanical complex as hybrid system, IEEE First Ukraine Conference on Electrical and Computer Engineering (UKRCON), Ukraine, 2017, pp. 399 – 404.

[2] Zablodskiy M, Zhiltsov A, Nalyvaiko V, et al., Biomass Pyrolysis Using a Multifunctional Electromechanical Converter and a Magnetic Field // Scientia agriculturae bohemica, 2020, Vol. 51(2), pp.65-73.

[3] Vencislav C. Valchev, Teodora P. Todorova, Dimitar D. Yudov and Daniela J. Mareva, Design considerations of inductors for induction heating of fluids, Electrical Apparatus and Technologies (SIELA) 2016 19th International Symposium on, 2016.

[4] Nemkov V.S., Demidovich V.B Theory and calculation of induction heating devices. Energoatomizdat (1988), 280 p. (Rus).

[5] Humphries S., Finite-element Methods for Electromagnetics. Electronic edition (2010), 329 p.

[6] Jankowski T.A., Pawley N.H., Gonzales L.M., Ross C.A., Jurney J.D. Approximate analytical solution for induction heating of solid cylinders // Appl. Math. Model., vol. 40, pp. 2770-2782, 2016.

[7] Zhiltsov A, Kondratenko I, Lyktei V., Usenko S., The magnetic field calculation in electromechanical systems with saturated ferromagnetic structural elements, *Przegląd Elektrotechniczny*, R.97, NR 1/2020, pp. 69-72.

[8] Kondratenko I, Zhiltsov A, Bereziuk A, Electromagnetic field of the three-phase cylindrical inductor if it runs off with frequency converter in non-stationary modes, IEEE International Young Scientists Forum on Applied Physics and Engineering (YSF), Ukraine, 2017, pp. 247-250.

[9] Bereziuk A, Karlov O, Kryshchuk R, et al., Improved method of calculation the electromagnetic generator for environmentally friendly method of forming coolant, 6th International Conference – Renewable Energy Sources (ICoRES), Poland, 2020, Vol. 154 № 04002.